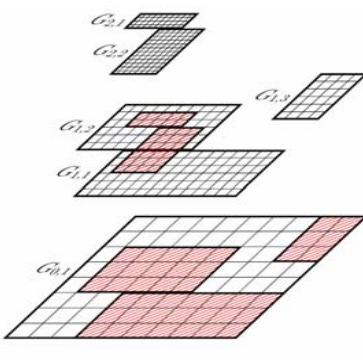


Abstract. We have developed a block-structured AMR framework that enables the coupled simulation of shock- and detonation-wave-driven fluid-structure interaction (FSI) problems. The approach is general and allows the incorporation of any computational solid mechanics (CSD) solver. The key idea of the system is to orchestrate the boundary data exchange between Lagrangian solid mechanics solvers and Eulerian fluid mechanics schemes through a ghost fluid approach in which complex embedded boundaries are implicitly represented with evolving level set functions. The level set information is updated on-the-fly.

Structured Adaptive Mesh Refinement (SAMR)

- Generic C++ implementation of the Berger-Colella SAMR algorithm for time explicit finite volume schemes
- Conservative correction for purely Cartesian problems
- Encapsulates dynamic mesh adaptation and parallelization to the fluid solver developer
 - Numerical scheme for only for single block necessary
- Large number of 3d patch discretizations available, e.g.
 - Second-order Riemann-solver for Euler equations with detailed chemistry



$$\frac{\partial \rho}{\partial t} + \frac{\partial}{\partial x_k}(\rho u_k) = 0$$

$$\frac{\partial}{\partial t}(\rho u_i) + \frac{\partial}{\partial x_k}(\rho u_i u_k + \delta_{ik} p) = 0$$

$$\frac{\partial E}{\partial t} + \frac{\partial}{\partial x_k}(u_k(E + p)) = 0$$

$$\frac{\partial}{\partial t}(\rho Y_i) + \frac{\partial}{\partial x_k}(\rho Y_i u_k) = \dot{m}_i$$

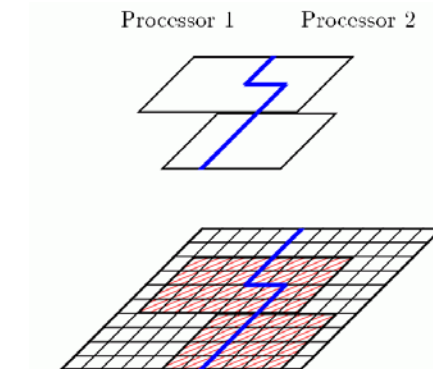
$$p = \rho R T \sum_{i=1}^N \frac{Y_i}{W_i}$$

$$\rho h - p - E + \frac{1}{2} \rho u_k u_k = 0$$

$$h = \sum_{i=1}^N h_i(T) Y_i$$

$$h_i(T) = h_i^0 + \int_{T_0}^T c_{pi}(T^*) dT^*$$

$$\dot{m}_i = W_i \sum_{j=1}^M (\nu_{ji}^r - \nu_{ji}^f) [k_j^f \prod_{n=1}^N (\frac{\rho_n}{W_n})^{\nu_{jn}^f} - k_j^r \prod_{n=1}^N (\frac{\rho_n}{W_n})^{\nu_{jn}^r}]$$

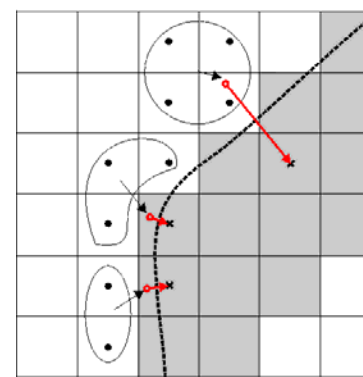


Current parallelization strategy

- Data of all levels resides on same node → Interpolation and averaging remain strictly local
- Only parallel operations to be considered:
 - Parallel synchronization as part of ghost cell setting
 - Load-balanced repartitioning of data blocks as part of regridding operation
 - Application of flux correction terms on coarse-grid cells
- Partitioning at root level with generalized Hilbert space-filling curve

Ghost-fluid method

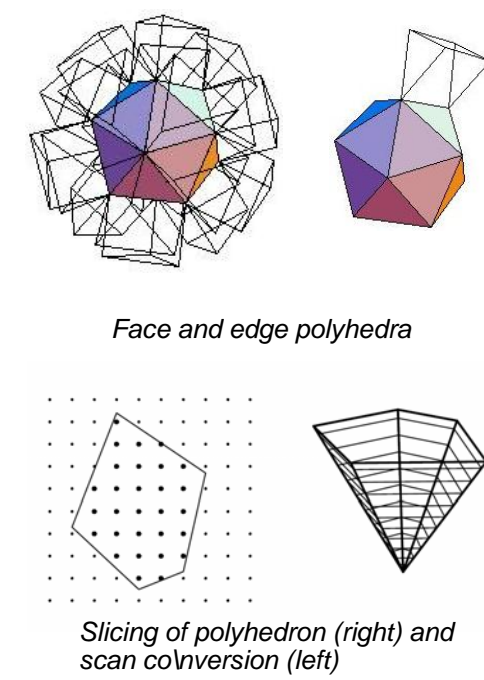
- Incorporate complex moving boundary/interfaces into any Cartesian solver by modifying cell values before update step
- Construction of values in embedded boundary cells by interpolation / extrapolation
- Implicit boundary representation via distance function ϕ , normal $n = \nabla \phi / |\nabla \phi|$
- Treat a fluid-solid interface as a moving rigid wall (requires mirroring of values at zero level set)
- Method diffuses boundary and is therefore not conservative
- Higher resolution at embedded boundary usually required than with first-order unstructured scheme
- Appropriate level-set-based refinement criteria are available



Interpolation stencil sizes for mirroring cell values into internal ghost cells (gray).

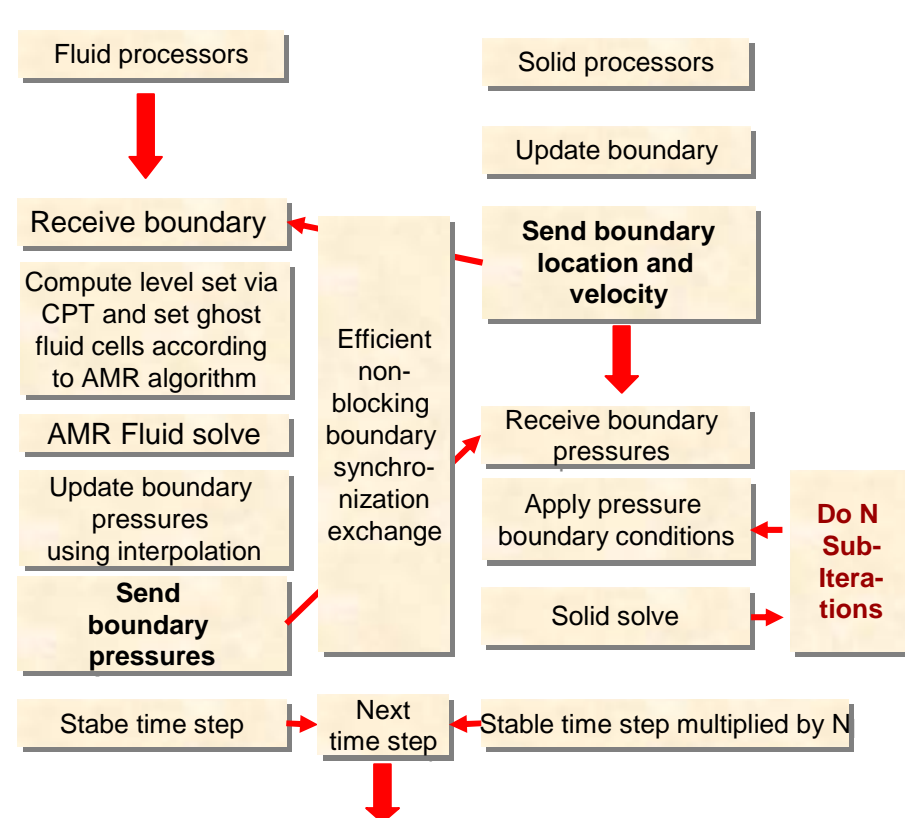
Level set computation

- For simple geometries with rigid body dynamics, distance function can be prescribed directly. For fully coupled FSI problems, the level set needs to be derived on-the-fly from an evolving surface mesh.
- Problem is equivalent to finding for each Cartesian grid point the closest element on the surface mesh
- Efficient algorithm based on reconstruction of characteristic polyhedra and scan conversion by S. Mauch (California Institute of Technology)
- Problem reduction by evaluation only within specified max. distance
- For each face/edge/vertex:
 - Scan convert the polyhedron
 - Find distance, closest point to that primitive for the scan converted points
- Computational complexity:
 - $O(m)$ to build the b-rep and the polyhedra.
 - $O(n)$ to scan convert the polyhedra and compute the distance, etc.



Fluid-Structure coupling

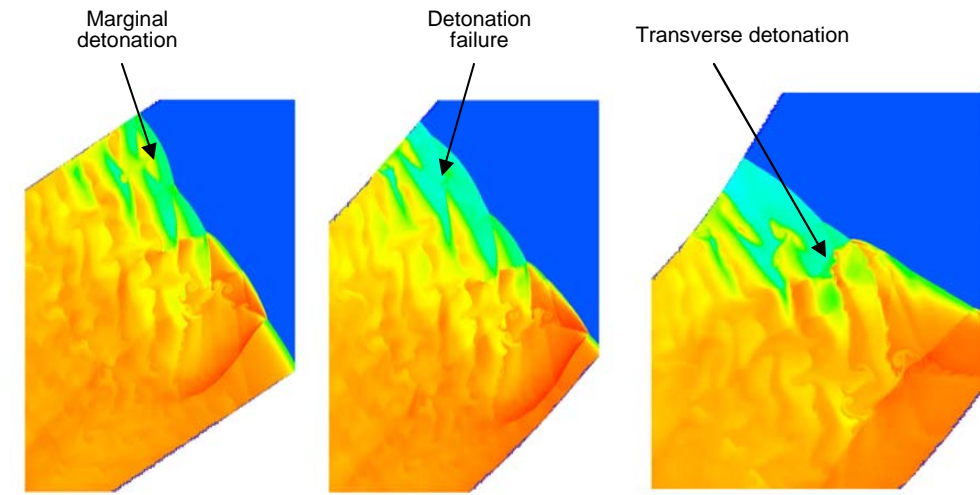
- Coupling of Euler equations for compressible flow to Lagrangian structure mechanics
- Compatibility conditions between inviscid fluid and solid at a slip interface
 - Continuity of normal velocity $u_n^s = u_n^f$
 - Continuity of normal stresses $\sigma_{nn}^s = -p^f$
 - No shear stresses $\sigma_{nt} = \sigma_{no} = 0$
- Interpolation operations with solid surface mesh
 - Mirrored fluid density and velocity values u^f into ghost cells
 - Solid velocity values u^s on facets
 - Fluid pressure values in surface points (nodes or face centroids)



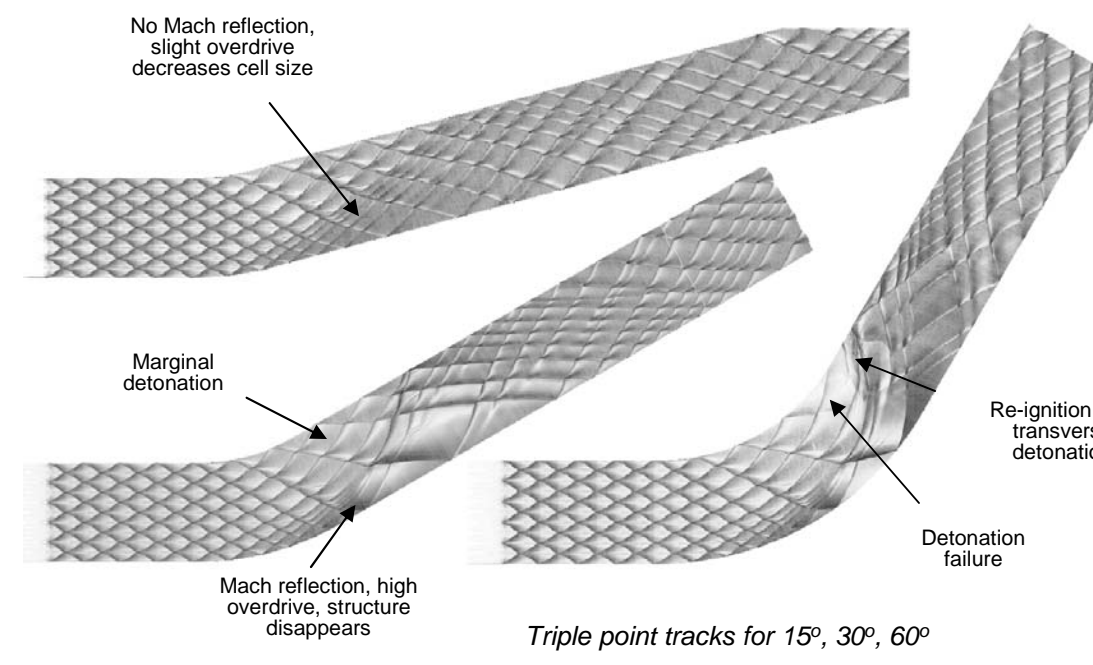
Right: Coupling algorithm: data exchange between dedicated fluid and solid processors.

Detonation propagation through smooth pipe bends

- Static level set prescribed directly
- Numerical investigation of detonation quenching and re-ignition in single configuration
- Study of the influence of structure (triple points)
- Regular oscillating Chapman-Jouguet detonation for $H_2 : O_2 : Ar : 2 : 1 : 7$ at $T_0 = 298K$ and $p_0 = 10kPa$, cell width 1.6 cm.
- Euler equations for 9 thermally perfect species, 34 elementary reactions
- Adaptation criteria:
 - Scaled gradients of ρ and p
 - Error estimation in Y_i by Richardson extrapolation
- 67.6 Pts within induction length. 4 additional refinement levels (2,2,2,4)
- Tube width of 5 detonation cells (8 cm).
- Pipe bend with same radius. Angle: 15°, 30°, 45°, 60°
- 67.6 Pts within induction length. 4 additional refinement levels (2,2,2,4). Adaptive computations use $\approx 7 \cdot 10^6$ cells ($\approx 5 \cdot 10^6$ on highest level) instead of $1.2 \cdot 10^9$ cells (uniform grid).
- Each run $\sim 70,000h$ CPU on 128 CPUs Pentium-4 2.2GHz of the ALC at LLNL

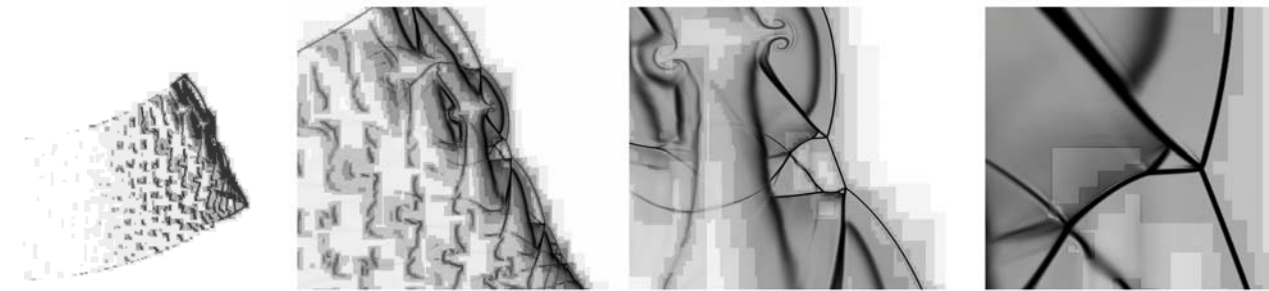


Temperature plots for 15°, 45°, 60° bending angle



Triple point tracks for 15°, 30°, 60°

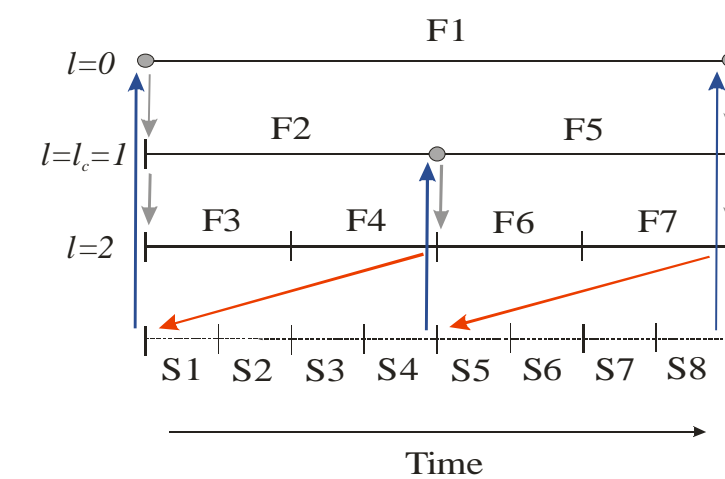
- Computational savings from SAMR: 250 up to 680
- Shock structure of double Mach reflections is resolved through entire simulation



Schlieren of density on refinement levels. Zoom into single triple point.

Coupling of Eulerian SAMR to a non-adaptive CSD solver

- Exploit SAMR time step refinement for effective coupling to solid solver
 - Lagrangian simulation is called only at level $l_c < l_{max}$
 - SAMR refines solid boundary at least at level l_c
 - One additional level reserved to resolve ambiguities in ghost fluid method (e.g. thin structures)
- Nevertheless: Inserting sub-steps accommodates for time step reduction from time-explicit CSD solvers within an SAMR cycle
- Communication strategy
 - Updated boundary info from solid solver must be received (blue arrow) before regridding operation (gray dots and arrows)
 - Boundary data is sent to solid (red arrow) when highest level available
- Inter-solver communication (point-to-point or globally) managed on-the-fly by non-blocking Eulerian-Lagrangian MPI Coupling module



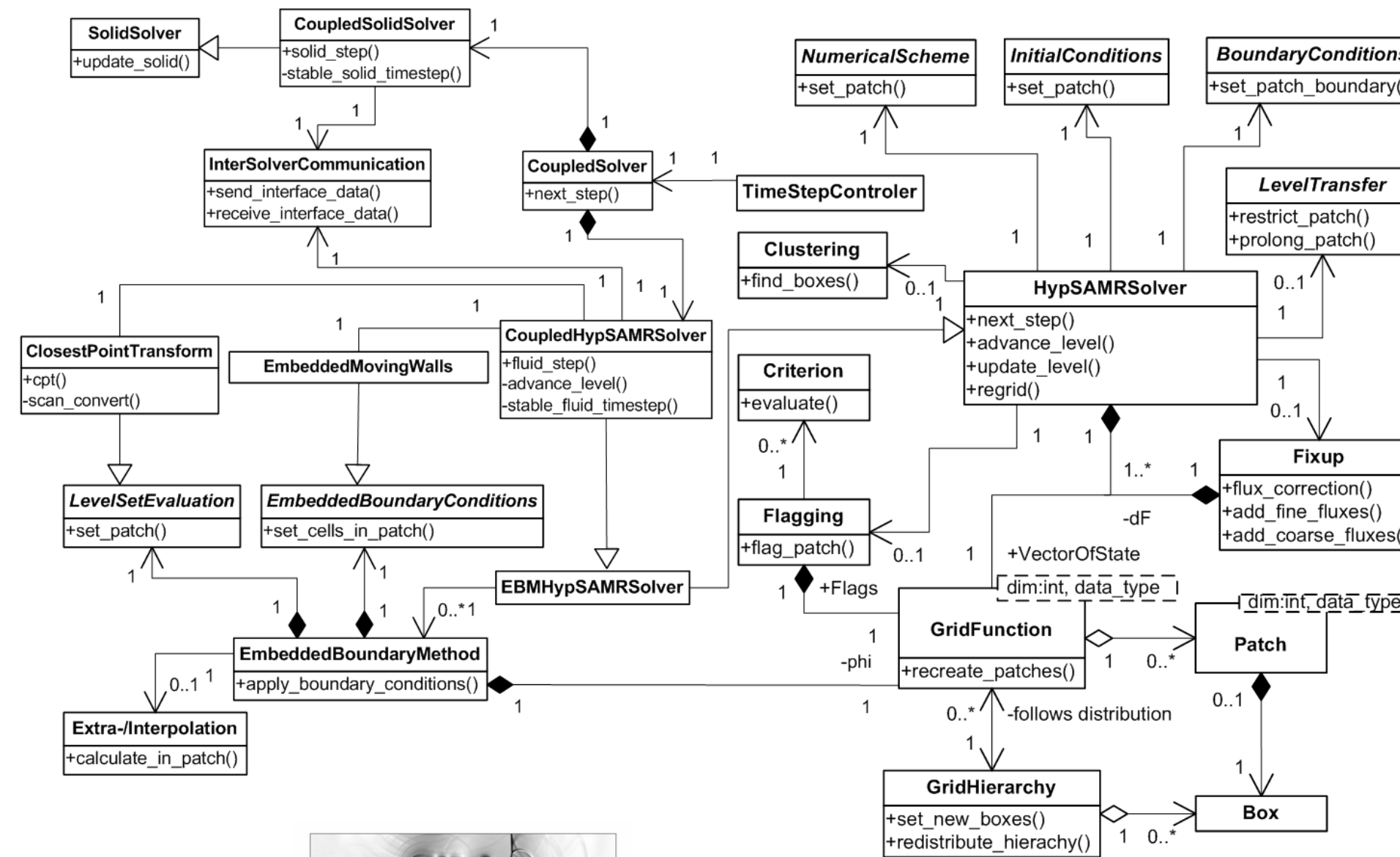
Fluid-structure data exchange incorporated into hierarchical SAMR time step refinement. Blue: send of pressure data, red: receive geometry and nodal velocities.

Software design

The VTF is constructed on top of the Amroc SAMR class hierarchy in a C++ framework approach.

- The design acknowledges the greater complexity on the Eulerian side in our coupling approach.
- Applications use one generic main program that instantiates predetermined objects.
- Objects can be extensively customized by C++ class derivation.
- Problem-specific routines (initial conditions, boundary conditions) are provided in F77/90 or C/C++.

UML class diagram for the VTF software. Right half: most important classes in Cartesian Amroc. Left side: Extensions for implementing the generic ghost fluid method and coupling with a CSD solver.



Shock-induced motion of a thin panel

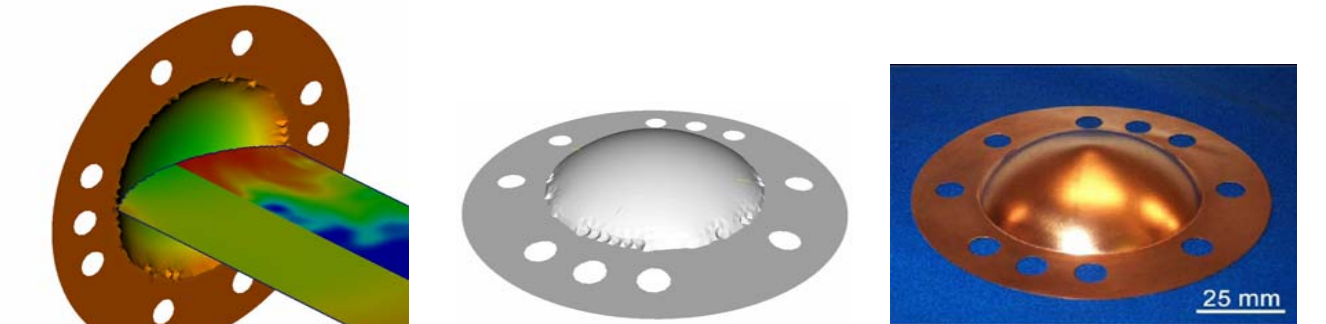
- Verification and demo simulation
- Mach-1.21 inflow in air ($\gamma=1.4$, $P_{CJ}=100kPa$, 293K) impinges on thin steel panel of 1mm thickness and 50mm length
- Fluid
 - Two-dimensional 0.4m x 0.08m flow domain with forward facing step geometry, reflective boundaries everywhere except inflow on left side.
 - AMR base mesh 320x64, 2 additional levels with factors 2, 4
- Solid – 1d beam solver using Euler-Bernoulli theory
 - 80 finite difference points in beam middle axis
 - Panel situated 1.5cm behind start of step, elastic material
- 4 nodes 3.4 GHz Intel Xeon dual processor, Gigabit Ethernet network, ca. 54h CPU (7 fluid processors, 1 solid processor)



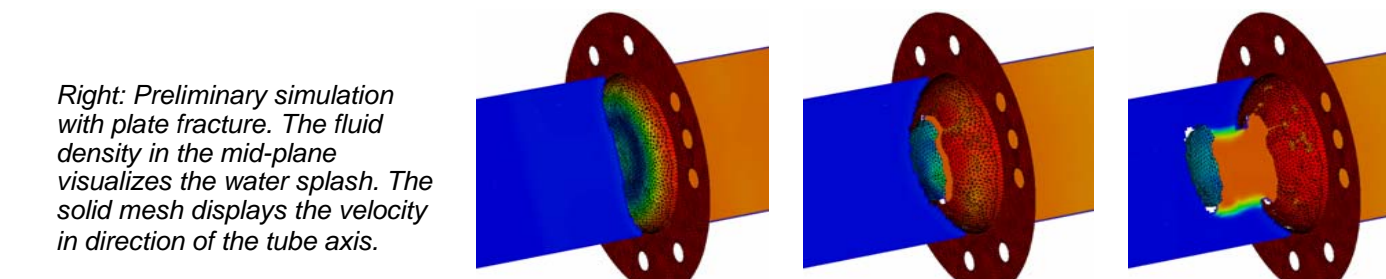
Right: Schlieren plot of fluid density in the vicinity of the thin steel panel. Snapshots for $t=0.51ms$, $1.63ms$, and $3.02ms$ (from top to bottom). Vortex shedding from panel tip and beam vibration induced by shock impact.

Water-hammer-driven plate deformation

- Piston-induced strong pressure wave in water shock tube impinges on thin copper plate.
- Correct pressure wave profile generated by propagating upper tube boundary according to equation of motion for piston
- Water shock tube of 1.3m length, 64mm diameter
- Two-component solver, modeling of water with stiffened gas equation of state with $\gamma=7.415$, $p_{\infty}=296.2 MPa$, air with ideal gas equation of state with $\gamma=1.4$
- AMR base level: 350x20x20, 2 additional levels, refinement factors 2, 2
- Approx. $1.2 \cdot 10^6$ cells used in fluid on average instead of $9 \cdot 10^6$ (uniform)
- Solid – Thin-shell finite element solver by F. Cirak (University Cambridge)
- Copper plate of 0.25mm thickness, J2 plasticity model with hardening, rate sensitivity, and thermal softening
- Shell mesh: 4675 nodes, 8896 elements
- Incorporate lower-dimensional boundary structure by treating cells with $0 < \phi < d$ as ghost fluid cells
- Unsigned distance level set function ϕ
- Leaving level set unmodified ensures correctness of $\nabla \phi$
- Use face normal in shell element to evaluate in $\Delta p = p^* - p$
- 8 nodes 3.4 GHz Intel Xeon dual processor, Gigabit Ethernet network, ca. 130h CPU



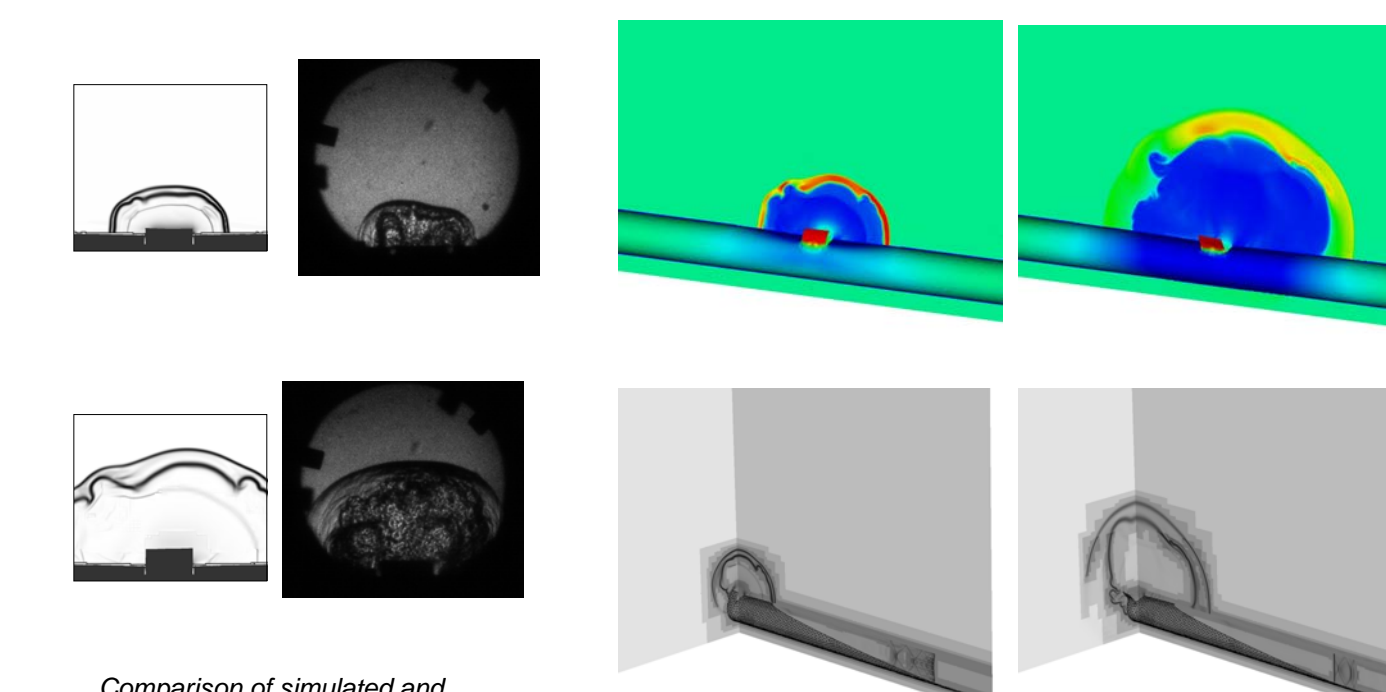
Left: velocity in direction of tube axis in plate and fluid (lower half of plane) and fluid pressure (upper half of plane) 1.62ms after piston impact. Right: plate at end of simulation and after experiment.



Right: Preliminary simulation with plate fracture. The fluid density in the mid-plane visualizes the water splash. The solid mesh displays the velocity in direction of the tube axis.

Elastic-plastic validation – Tube with flaps

- Fluid
 - Constant volume burn model with $\gamma=1.24$, $P_{CJ}=3.3 MPa$, $D_{CJ}=2376 m/s$
 - AMR base level: 104x80x242, 3 additional levels, factors 2,2,4
 - Approx. 40M cells instead of 7,930M cells (uniform)
 - Tube and detonation fully refined
 - Thickening of 2d mesh: 0.81mm on both sides (real thickness on both sides 0.445mm)
 - 16 nodes 2.2 GHz AMD Opteron quad processor, PCI-X 4x Infiniband network
- Solid
 - Aluminum, J2 plasticity with hardening, rate sensitivity, and thermal softening from Adlib material library
 - Mesh: 8577 nodes, 17056 elements
 - 16+2 nodes 2.2 GHz AMD Opteron quad processor, PCI-X 4x Infiniband network
 - Ca. 4320h CPU to $t=450 \mu s$

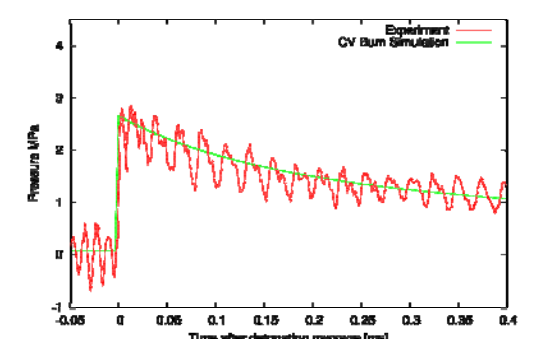


Comparison of simulated and experimental Schlieren images.

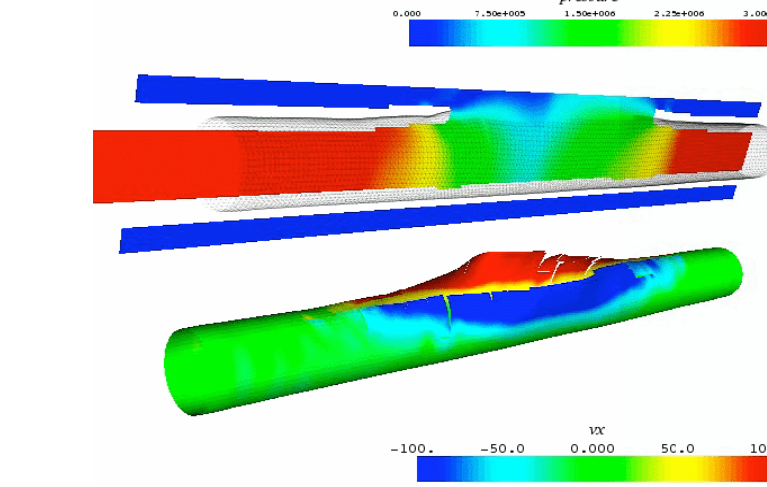
Top: Color plot of fluid density and solid displacements in y-direction. Bottom: Schlieren images of density on refinement levels show the dynamic mesh adaptation in the fluid domain.

Detonation-driven fracture of thin aluminum tubes

- Motivation: Complex fluid-structure interaction problem
- Interaction of detonation, ductile deformation, fracture
- Fluid
 - Constant volume burn model with $\gamma=1.24$, $P_{CJ}=6.1 MPa$, $D_{CJ}=2402m/s$ (Right: flow field before specimen)
 - 40x40x725 cells unigrid
- Solid – Thin-shell FEM solver with fracture and fragmentation capability by F. Cirak (University Cambridge)
 - Shell mesh: 206,208 nodes
 - Material model for cohesive interface element: linearly decreasing envelope
 - 972h CPU with 33 shell and 21 fluid processors on ALC at LLNL



Fluid solver initial conditions derived from one-dimensional shocktube simulation.



Coupled simulation of detonation-driven rupture 0.260 ms after the detonation has passed the initial notch.

Acknowledgements. This work is sponsored by the Office of Advanced Scientific Computing Research; U.S. Department of Energy (DOE) and was performed at the Oak Ridge National Laboratory, which is managed by UT-Battelle, LLC under Contract No. DE-AC05-00OR22725. Part of this work was also performed at the California Institute of Technology and was supported by the ASC program of the Department of Energy under subcontract No. B341492 of DOE contract W-7405-ENG-48.